Author/s:
Quek, C;Bellingham, SA;Jung, CH;Scicluna, BJ;Shambrook, MC;Sharples, RA;Cheng, L;Hill, AF

Title:
Defining the purity of exosomes required for diagnostic profiling of small RNA suitable for biomarker discovery

Date:
2017-02-01

Citation:
Quek, C., Bellingham, S. A., Jung, C. H., Scicluna, B. J., Shambrook, M. C., Sharples, R. A., Cheng, L. & Hill, A. F. (2017). Defining the purity of exosomes required for diagnostic profiling of small RNA suitable for biomarker discovery. RNA Biology, 14 (2), pp.245-258. https://doi.org/10.1080/15476286.2016.1270005.

Persistent Link:
https://hdl.handle.net/11343/257676

RNA BIOLOGY
2017, VOL. 14, NO. 2, 245–258
http://dx.doi.org/10.1080/15476286.2016.1270005

Taylor & Francis
Taylor & Francis Group

RESEARCH PAPER

OPEN ACCESS

Defining the purity of exosomes required for diagnostic profiling of small RNA suitable for biomarker discovery

Camelia Quek [a,b,*], Shayne A. Bellingham[a,*], Chol-Hee Jung [c], Benjamin J. Scicluna[a,b], Mitch C. Shambrook[b], Robyn A. Sharples[a], Lesley Cheng[b], and Andrew F. Hill [b]

[a]Department of Biochemistry and Molecular Biology, Bio21 Molecular Science and Biotechnology Institute, University of Melbourne, Melbourne, VIC, Australia; [b]Department of Biochemistry and Genetics, La Trobe Institute for Molecular Science, La Trobe University, VIC, Australia; [c]VLSCI Life Sciences Computation Centre, University of Melbourne, VIC, Australia

ABSTRACT

Small non-coding RNAs (ncRNA), including microRNAs (miRNA), enclosed in exosomes are being utilised for biomarker discovery in disease. Two common exosome isolation methods involve differential ultracentrifugation or differential ultracentrifugation coupled with Optiprep gradient fractionation. Generally, the incorporation of an Optiprep gradient provides better separation and increased purity of exosomes. The question of whether increased purity of exosomes is required for small ncRNA profiling, particularly in diagnostic and biomarker purposes, has not been addressed and highly debated. Utilizing an established neuronal cell system, we used next-generation sequencing to comprehensively profile ncRNA in cells and exosomes isolated by these 2 isolation methods. By comparing ncRNA content in exosomes from these two methods, we found that exosomes from both isolation methods were enriched with miRNAs and contained a diverse range of rRNA, small nuclear RNA, small nucleolar RNA and piwi-interacting RNA as compared with their cellular counterparts. Additionally, tRNA fragments (30–55 nucleotides in length) were identified in exosomes and may act as potential modulators for repressing protein translation. Overall, the outcome of this study confirms that ultracentrifugation-based method as a feasible approach to identify ncRNA biomarkers in exosomes.

ARTICLE HISTORY
Received 15 August 2016
Revised 21 October 2016
Accepted 1 December 2016

KEYWORDS
Biomarkers; exosomes; miRNA; small RNA

Introduction

Small RNAs are non-coding RNAs (ncRNAs) that are approximately 18–250 nucleotides (nt) in length.[1,2] which can finely control the expression of target genes that control diverse biologic processes, such as proliferation, development, differentiation and apoptosis[3-6] The common ncRNA species include microRNA (miRNA), piwi-interacting RNA (piRNA), rRNA (rRNA), tRNA (tRNA), small nuclear RNA (snRNA) and small nucleolar RNA (snoRNA).[7]

The role of small RNAs as potential modulators in diseases has been increasingly recognized and there is now a significant interest in using exosomes to identify small RNA biomarkers for diagnosis of disease such as neurodegenerative diseases,[8-10] cancer[11-13] and autoimmune disease.[14,15] Small RNAs can be secreted in cell-derived extracellular vesicles such as exosomes as a method of intercellular communication.[16] Both mRNA and miRNA species have been found contained in exosomes which are taken up by specific target cells to facilitate disease spreading and pathogenesis.[17] As such, exosomes can provide a means for transfer and protection of RNA content from degradation in the environment, enabling a stable source for reliable detection of RNA biomarkers.[18,19]

To study exosomes and their ncRNA content, there are various methods available to isolate exosomes before performing downstream analysis such as next-generation sequencing (NGS).[20-22] The most common method to isolate exosomes is differential ultracentrifugation (UC), however this method may also isolate microvesicles or other particles/debris of similar sizes.[23,24] Optiprep velocity gradient ultracentrifugation has been shown to isolate a higher purity of exosomes as it can separate buoyant vesicles with similar physical properties.[23,24] For these reasons, Optiprep velocity gradient ultracentrifugation has increasingly become a preferred choice for exosome isolation when investigating the function and transfer of exosomal material devoid of possible contamination of other extracellular vesicles. Unfortunately, preparing gradients can be time consuming and may not be required for all areas of exosomal research. It has been debated whether the additional step of using Optiprep velocity gradients is required for biomarker

CONTACT Andrew F. Hill andrew.hill@latrobe.edu.au Department of Biochemistry and Genetics La Trobe Institute for Molecular Science La Trobe University Kingsbury Drive, Victoria 3086, Australia.
Supplemental data for this article can be accessed on the publisher's website.
*These authors contributed equally to this work.

discovery work and diagnostic testing, areas which efficiency and reproducibility are the important factors.

Upon the isolation of exosomes, there are many methods to profile RNA in exosomes, ranging from microarrays, or quantitative reverse transcription polymerase chain reaction (qRT-PCR) to NGS.[25] Most of the existing tools (e.g. qRT-PCR and microarray) offer high sensitivity and specificity in small RNA research, however they are unable to accurately detect a wide spectrum of ncRNAs. These methods typically require prior knowledge of the sequence of interest to design primers.[26] NGS technology does not require any prior knowledge of ncRNAs and thus it allows all ncRNA species to be sequenced in a high throughput manner.[27]

In this study we used, mouse hypothalamic neuronal (GT1–7) cells which have been widely used to study neuronal exosomes in neurodegenerative diseases, particularly prion disease.[23,29,41] Using GT1–7 cells, we evaluate the two widely used techniques for profiling small RNAs in exosomes; (i) differential UC and (ii) Optiprep velocity gradient ultracentrifugation. We investigated if there are any differences in the small RNA profiles of highly purified exosomes by using a high throughput workflow, which we developed for rapid and accurate profiling of small RNA.[28] Using the high throughput workflow, small RNAs, including miRNA, piRNA, rRNA, tRNA, snRNA, snoRNA and protein-coding mRNA fragments, are comprehensively surveyed in neuronal exosomes prepared by the two isolation methods. The findings present a high coverage approach for determining the optimal exosomes isolation method for small RNA profiling.

Material and methods

Cell culture

Mouse hypothalamic neuronal GT1–7 cell lines were cultured in Opti-MEM (Life Technologies, Melbourne, VIC, Australia) supplemented with 1 × GlutaMax (Life Technologies), 10% fetal calf serum (FCS) (Life Technologies) and 100 μg/ml penicillin/streptomycin and maintained at 37°C in 5% CO_2.

Exosome isolation

GT1–7 cells (~1 × 10^7 cells or 3 × T175 flasks) were cultured in exosome-depleted medium (complete medium containing exosome-free FCS) for 4 d. Exosomes were isolated using two exosome isolation methods (Fig. 1A and B). Protocol 1: Exosomes were isolated using the differential UC protocol as described previously.[29] Briefly, cultured supernatants were collected and centrifuged at 3,000 g for 10 min to remove cell debris. The supernatant was filtered (0.22 μm), and filtrate was centrifuged at 10,000 g for 30 min at 4°C. The supernatant was collected and exosomes were pelleted by centrifugation at 100,000 g(av). Exosome pellets were washed in filtered phosphate-buffered saline (PBS) and re-centrifuged at 100,000 g (av). The final exosome pellet was re-suspended in 100 μL filtered PBS; 50 μL was used for exosome characterization and remaining 50 μL was used for small RNA extraction. Protocol 2: Exosomes were isolated using Optiprep velocity gradient centrifugation protocol as described previously.[23] The steps were similar to the above described differential UC method in protocol 1 except that the initial 100,000 g pellet was re-suspended in 500 μl NTE buffer (137 mM NaCl, 1 mM EDTA, and 10 mM Tris, pH 7.4). Exosome suspension was layered on a 10-mL continuous 10–30% Optiprep gradient made up in NTE buffer and centrifuged at 250,000 g, 1.5 h, 4°C. From top of the gradient, 17 fractions (600 μL) were collected; 300 μL was used for exosome characterization and remaining 300 μL was used for small RNA extraction.

Size distribution analysis

Tunable resistive pulse sensing analysis was performed using the qNano system (Izon, Christchurch, New Zealand); by applying a voltage and pressure, single particles are passed through a stretched polyurethane nanopore. As the particle traverses the pore, ions are occluded resulting in a drop in the measured current, termed a 'blockade event'. Exosome samples and calibration particles of known size were analyzed in PBS on a NP-150 nanopore. Each sample was measured with applied pressures of 8 and 12 cmH2O, for multi-pressure calibration, where measurement consisted of a minimum of 500 blockade events.

Transmission electron microscopy

Exosomes were fixed with 2% glutaraldehyde/PBS for 30 min at room temperature. A volume of 6 μl was applied to a glow-discharged 200-mesh Cu grid coated with carbon-Formvar film (ProSciTech, Kirwan, QLD, Australia) and allowed to absorb for 5 min. Grids were washed twice with Milli-Q water and contrasted with 1.5% uranyl acetate. Transmission electron microscopy (TEM) was performed on a Tecnai G2 F30 (FEI, Eindhoven, NL) TEM operating at 300 kV across × 15,000 to × 36,000 magnification. Electron micrographs were captured with a Gatan UltraScan® 1000 2 k × 2 k CCD camera (Gatan, Pleasanton, CA).

Western immunoblotting

Cell lysates and exosome samples were lysed in sodium dodecyl sulfate (SDS) sample buffer (2% (w/v) SDS, 10% (v/v) glycerol, 12.5mM ethylenediaminetetraacetic acid, 2 mg Bromophenol blue, 50mM Tris pH 6.8) with 5% ß-mercaptoethanol and heated at 95°C. The lysed samples were subjected to electrophoresis using precast Novex 4–12% Bis-Tris NuPAGE gels (Invitrogen). Proteins were electrotransferred onto polyvinylidene difluoride (PVDF) membranes using the Criteron Transfer system (Bio Rad, Hercules, CA, USA). The PVDF membranes were blocked with 5% (w/v) skim milk powder in PBS containing 0.05% Tween-20 (PBS-T) at room temperature. Membranes were probed with the following antibodies and working dilutions: anti-tsg101 (Santa Cruz Biotechnology, CA, USA) at 1:3000, anti-Bcl2 (BD Biosciences, Sydney, NSW, Australia) at 1:1000, anti-flotillin-1 (BD Biosciences, Sydney, NSW, Australia) at 1:3000, anti-SAF-32 (Prion protein) at 1:5000 (Sapphire Biosciences, Redfern, NSW, Australia) anti-mouse HRP (GE Healthcare, Sydney, NSW, Australia) at 1:25,000 and anti-goat HRP (Sigma-Aldrich, Sydney, NSW, Australia) at

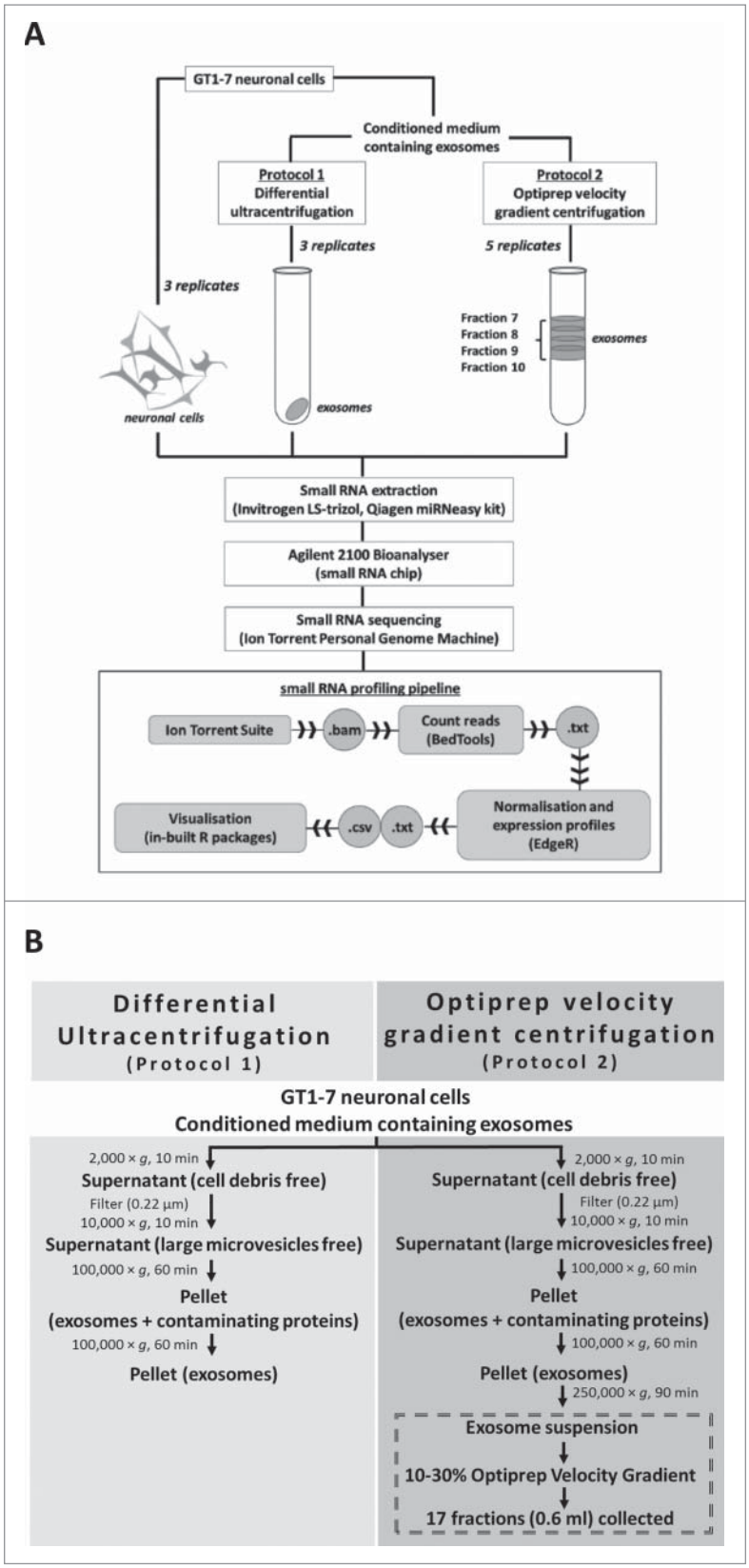

Figure 1. Workflow outlining the exosomal small RNA sequencing experiment and data analysis. (A) Exosomes released from GT1–7 neuronal cells found in the conditioned media were isolated using 2 different centrifugation-based protocols. Protocol 1 involves the use of differential UC and Protocol 2 involves isolating exosomes using differential UC over a continuous 10–30% Optiprep gradient. Upon exosome isolation small RNA was extracted from both cells and exosomes using TRIzol-LS followed by clean up using the column-based miRNeasy kit. The quality and quantity of the small RNA were checked by Agilent 2100 Bioanalyser. Libraries were constructed and subjected to small RNA transcriptome sequencing using Ion Torrent Personal Genome Machine. The initial bioinformatics analysis of pre-processing, quality assessment and sequence mapping (i.e. TMAP) were performed in Ion Torrent Suite. The generated high quality and aligned data was subjected to an in-house developed small RNA analysis pipeline that integrates BEDtools and edgeR for small RNA profiling. The pipeline automatically generates output of raw counts, normalized counts and vizualization graphics including, but not limited to, hierarchical clustering heatmap and multidimensional scaling. (B) Flowchart describing the steps of the 2 protocols used to isolate exosomes from the conditioned medium; (i) differential UC and (ii) Optiprep velocity gradient ultracentrifugation.

1:100,000. Immunoreactive bands were detected using the enhanced Chemiluminescence kit (Amersham Biosciences, Rydelmere, NSW, Australia) followed by exposed to Hyperfilm (Amersham) and developed by Exomat automated developing system.

Small RNA Extraction

The total RNA including miRNA from exosome suspensions was extracted using a column-based miRNeasy kit (Qiagen, Chadstone, VIC, Australia) with the following modifications to the manufacturer's instructions. TRIzol-LS (Life Technologies), instead of QIAzol, was added to the exosome suspensions and subsequently vortexed. After incubation, chloroform was added to the homogenate and the manufacturer's protocol of the miRNeasy kit was resumed to isolate RNA sized between 18nt and above. The quantity and quality of the small RNA extractions were determined using a BioSpec-nano (Shimadzu, Rowville, VIC, Australia) and Agilent Bioanalyser 2100 with a small RNA assay Chip for cell-free exosomal small RNA, and a RNA Nano 6000 assay Chip for cellular RNA (Agilent Technologies, Mulgrave, VIC, Australia).

Small RNA library construction and Ion Torrent sequencing

Small RNA library preparation was performed using the Ion Total RNA-Seq kit v2 (Life Technologies) for both exosome samples and GT1–7 neuronal cell samples: a total of 26 libraries including replicates (see Results for details). For each individual library, RNA was ligated to adapters containing a unique index barcode (Ion Xpress™ RNA-Seq Barcode 1–16 Kit, Life Technologies) to allow libraries to be pooled during Ion Torrent sequencing (Life Technologies). All libraries were constructed according to manufacturer's protocol. Briefly, RNA samples were reverse transcribed to cDNA using adaptor specific primers. Using the Magnetic Bead Purification Module (Life Technologies), cDNA samples were size-selected from 94 to 200 nt (the length of the small RNA insert including the 3′ and 5′ adaptors). PCR amplification was then performed followed by a library clean-up step using nucleic acid beads (Life Technologies). The quality and quantity of each library were determined by Agilent 2100 Bioanalyser using High Sensitivity DNA kit (Agilent Technologies). Equally pooled libraries were clonally amplified onto Ion Sphere™ Particles (ISPs) supplied by the Ion PGM™ Template OT2 200 kit (Life Technologies). ISP templates were produced by using the OneTouch™ 2 Instrument and enrichment system (Life Technologies). ISPs loaded with libraries were sequenced on the Ion Torrent PGM™ using Ion™ 318 v2 chips (Life Technologies) and the Ion PGM™ 200 Sequencing Kit v2 (Life Technologies).

Small RNA sequence data analysis

Raw reads generated by sequencing were subjected to pre-processing, quality assessment and mapping using the default parameters provided in the Ion Torrent Suite (version 4). Briefly, the Ion Torrent Suite filtered for high quality reads by removal of adaptor sequences, low quality bases at 3′ ends of reads, adaptor dimers, reads lacking sequencing key, reads with low signal and polyclonal reads. The high quality reads were mapped to mm10 build of the mouse genome from University of California Santa Cruz (UCSC) genome databases using Torrent Mapping Alignment Program (TMAP) with their default parameters.

Aligned reads were classified according to genomic loci annotations using BEDtools. For instance, miRNA reads were identified by intersecting the genomic coordinates of aligned reads with those of known miRNA from miRBase release 20.[30] Subsequently, additional intersection to the other non-coding small RNAs was also performed in respect to their specific databases, including Genomic tRNA database[31] for tRNAs, piRNA Bank[32] for piRNAs and Ensembl for other classes of small RNAs (i.e. snoRNA, snRNA and rRNA). Reads that were not identified as known small RNAs were intersected with repeat elements and protein-coding mRNA retrieved from UCSC database. These intersection results were converted to read-count tables containing raw counts of each RNA biotype, which were analyzed and visualised using R-packages such as 'edgeR'[33] and 'pheatmap'.[34] This analysis workflow (Fig. 1A) was integrated into a pipeline developed in-house with python,[28] and the full details of the pipeline are described in Supplementary Methods. Calculation of percentage of reads by biotype was based on raw read counts of perfectly intersected and matched transcripts for each biotype compared with the total reads for each library. Sequences were deposited into European Nucleotide Archive[35] under accession number PRJEB9472.

Small RNA data output vizualization

Circos[36] was used to visualize the distribution of small RNAs from different data sets across chromosomes. Cytogenetic bands and chromosome labels were included to highlight the genomic location of small RNAs. In addition, the relationship of the replicates among the data sets was further analyzed using principle component analysis (PCA) and multidimensional scaling (MDS) in R.[33,34] The 'tune.pca' function[34] was initially performed to visualize the proportion of explained variance for selecting the final principal components.[37,38] The several intercorrelated variables across the replicates were represented in a 3-dimentional (3D) plot. Further, proportional 2-set Venn and 5-set Venn diagrams were performed to identify unique and common RNA biotypes using the respective 'Venneuler'[39] and 'gplots'[40] in R. The elements in each data set were compared with determine the intersection and union regions.

miRNA qRT-PCR and digital PCR assays

Individual qRT-PCR and digital PCR TaqMan® miRNA assays (Applied Biosystems) for let-7b (TaqMan® Assay ID 000378) and miR-342–3p (TaqMan® Assay ID 002260) were performed according to the manufacturer's instructions. The same amount of total RNA isolated from cells and exosomes was converted to cDNA using the miRNA reverse transcriptase Kit (Applied Biosystems) and specific miRNA assay RT primers. For qRT-PCR, cDNA was diluted 1:3 and setup in quadruplicate reactions in 96-well plates containing specific TaqMan® miRNA assays, and Fast TaqMan® Fast Advanced Master Mix in a final

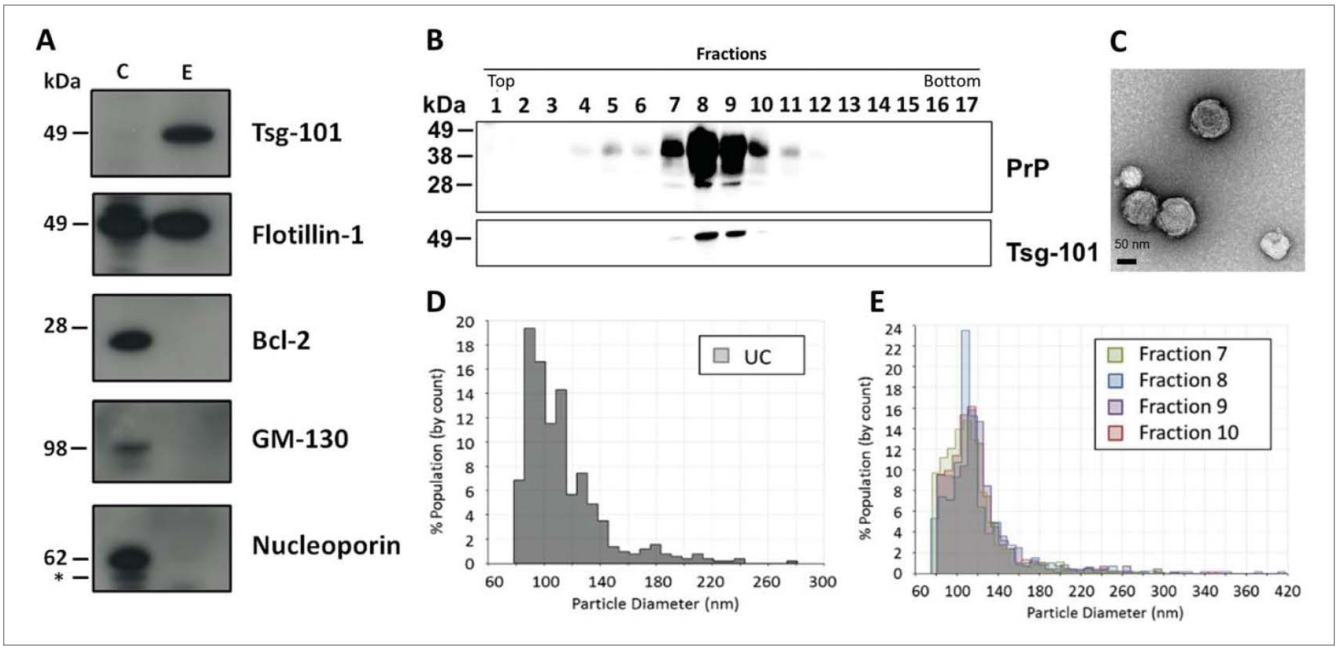

Figure 2. Characterization of exosomes and exosomal RNA content. (A) Western blot of GT1–7 cell lysates and exosomes isolated by differential UC was confirmed by enrichment of exosomes markers tsg-101 and flotillin-1, and absence of bands for negative markers Bcl2 (apoptotic bodies), GM-130 (Golgi apparatus), nucleoporin (nucleus). Abbreviations: kDa (kiloDalton); (C)(GT1–7 neuronal cells); (E)(exosomes). '*' denotes non-specific band for anti-nucleoporin. (B) Isolation of exosomes using Optiprep velocity gradient ultracentrifugation show the co-fractionation of exosomes whereby fractions ($n = 17$) were probed for the prion protein and exosome marker tsg-101. (C) Transmission electron microscope image of typical exosomes in fraction 8 isolated by Optiprep gradient. Size distribution histogram of exosomes normalized to exosome count analyzed by the qNano instrument; (D) Isolated by differential UC, (E) exosomes present in Optiprep fractions 7, 8, 9 and 10.

volume of 20 μl using the QIAGILITY liquid handing robot (QIAGEN). The qRT-PCR assay was run on a ViiA7 qRT-PCR instrument (Applied Biosystems) using the manufacturer's recommended cycling conditions. Data were plotted as raw cycle threshold (Ct) values. For digital PCR, cDNA was diluted 1:10 and set-up in duplicate reactions containing the specific TaqMan® miRNA assay and digital PCR master mix which was subsequently loaded and sealed into a QuantStudio™ 3D Digital PCR 20K Chip using QuantStudio™ 3D Digital PCR Chip Loader (Applied Biosystems), according to the manufacturer's instructions. The prepared digital PCR 20K Chips were loaded into the GeneAmp® PCR System 9700 (Applied Biosystems) and initiated the reaction using the manufacturer's recommended cycling conditions. The digital PCR 20K chips were then analyzed on the QuantStudio™ 3D PCR Instrument (Applied Biosystems) and were processed using QuantStudio® 3D AnalysisSuite™ for absolute quantification of miRNA targets in copies per μl.

Statistical analysis

Comparison of small RNA expression across different data sets was analyzed using Spearman's correlation between small RNA data sets in R. Other general statistics including median and mean ± SD were done using GraphPad Prism v5 (GraphPad Software).

Results

Characterization of neuronal cell-derived exosomes

Exosomes were isolated from GT1–7 cells using UC and Optiprep velocity gradient ultracentrifugation (Fig. 1A and B). The presence of exosomes was determined by Western blotting with a panel of antibodies for endosomal, plasma membrane, nuclear, Golgi and mitochondrial markers (Fig. 2A). Exosomes were enriched in tsg-101 and flotillin-1 while no detectable GM130, nucleoporin or Bcl^{-}2 was present. This observation indicates that exosome preparations were enriched in proteins of endosomal origin and that no contaminating nuclear, Golgi, mitochondrial and apoptotic membranes were present. Exosomes isolated by the Optiprep method were further probed with prion protein (PrP) and tsg-101 to indicate the presence of respective prion and exosomes after gradient separation (Fig. 2B).[23] Western blotting of Optiprep gradient fractions highlighted that fraction 8 and 9 were enriched with exosomes. Results from electron microscopy (Fig. 2C) and qNano (Fig. 2D and E) demonstrated that exosomes isolated from GT1–7 cells were composed of extracellular vesicles of ~100 nm in size. The morphology and size of vesicles were consistent with our previous studies using differential UC with or without Optiprep density gradients.[8,23]

Exosomes released from mouse GT1–7 hypothalamic neuronal cells contain RNA

RNA was extracted from neuronal cell-derived exosomes prepared by the 2 isolation methods (Fig. 1B) and the corresponding GT1–7 cells as a control. The quality and quantity of the isolated RNA were determined using an Agilent Bioanalyser, which showed an electropherogram of enriched RNA in Optiprep fractions 7–11 (Fig. S1A). The amounts of small RNA, including miRNA, peaked at fraction 8 ($\text{range}_{\text{miRNA}}$ = 2.14–2.66 ng/μl, $\text{median}_{\text{miRNA}}$ = 2.49 ng/μl; $\text{range}_{\text{smallRNA}}$= 20.5–

28.5 ng/μl, median$_{smallRNA}$= 27.2 ng/μl) and small RNA amounts (Fig. S1B) correlate with enriched exosomes as observed via Western blotting (Fig. 2B). Small RNA Bioanalyser profiles for exosomes isolated from either isolation method indicated that UC and fractions 8 and 9 contained high yield of RNA and a broad range of small RNA sizes between 4 and 100 nt in length, with an enriched peak at ~60 nt (Fig. S1C). Optiprep fractions 7 and 10, contained lower amounts of small RNAs, with the remaining fractions contained little or no small RNA.

Small RNA sequencing reads

To further investigate the presence of small RNA species, the Ion Torrent sequencing platform was used to perform unbiased deep sequencing of each sample. Based on the small RNA Bioanalyser profiles, Optiprep fractions 7, 8, 9 and 10 were selected for sequencing. Small RNA libraries were subsequently prepared for 6 data sets, with 5 replicates for Optiprep fractions 7–10 and 3 replicates for UC exosome and GT1–7 cell. The same amount of RNA (20 ng) across all samples was used for small RNA library construction. Read length distribution after adaptor removal revealed 3 major peaks at 18–22, 30 and 55 nt (Fig. 3). The peak at 18–22 nt indicates an abundance of mature miRNAs in exosomes and cells. After sequence alignment, an average of 1 × 10^6 sequencing reads was obtained (Supplementary Table S1).

Identification of different RNA biotypes via small RNA profiling pipeline

Small RNA species were identified using in-house small RNA analysis pipeline[28] that integrates BEDtools and edgeR as outlined in Supplementary Methods. The analyzed data sets contained a wide array of small RNAs across all the chromosomes (Fig. 4A). The composition of small RNA libraries (Fig. 4B) revealed that Optiprep and differential UC exosomes are comprised of miRNA (median 1.29%, range 0.48–2.11%), piRNA (median 1.09%, range 0.46–1.71%), snRNA (median 0.17%,

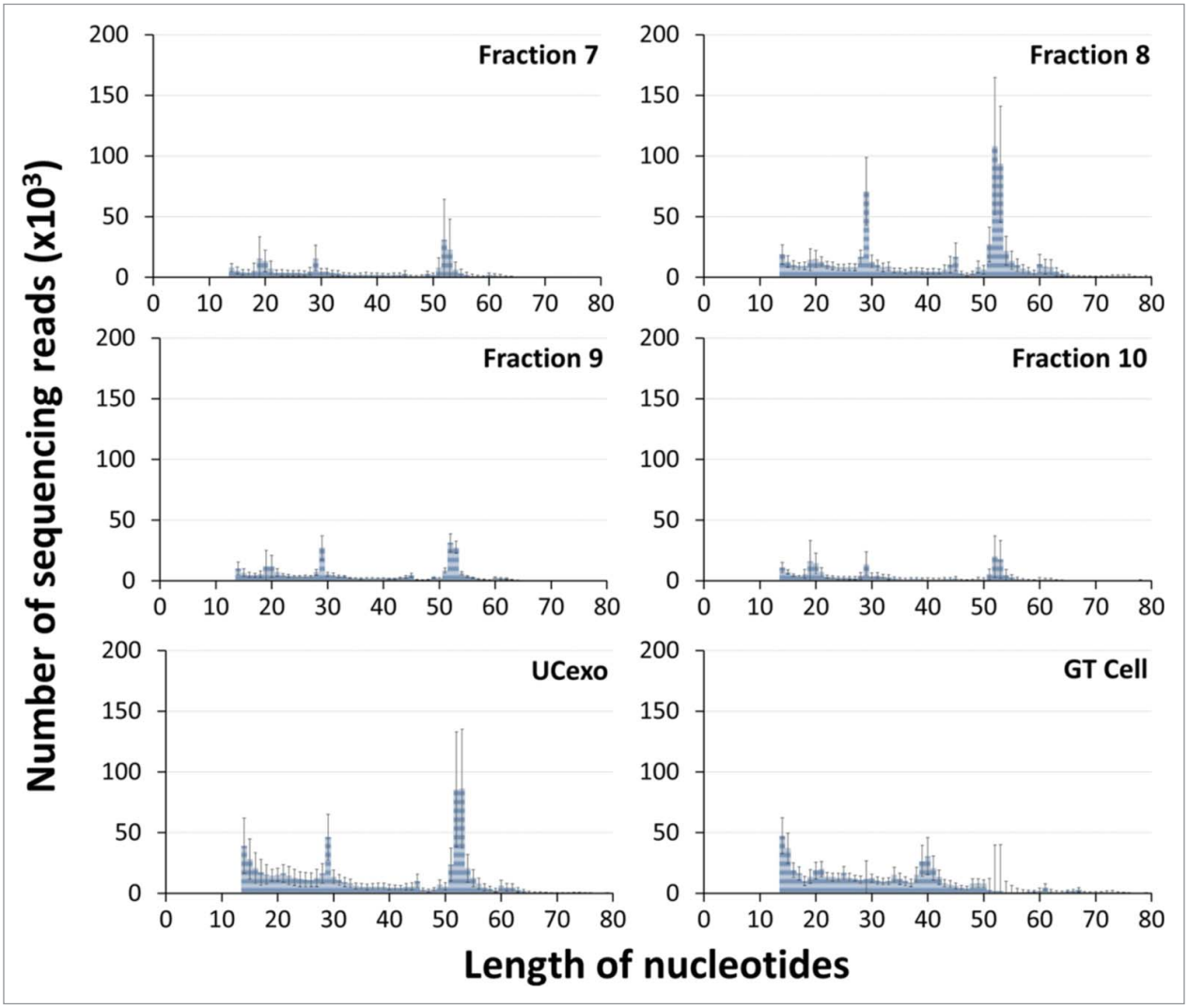

Figure 3. Read length of small RNA sequencing. Read length (nucleotide) distribution after adaptor removal. Each y-axis depicts the number of sequencing reads of all samples comprising of 5 replicates in each of the respective fraction, 3 replicates of exosomes isolated from ultracentrifugation method, and 3 replicates of GT1–7 neuronal cells. Standard deviations are shown in the bar graph.

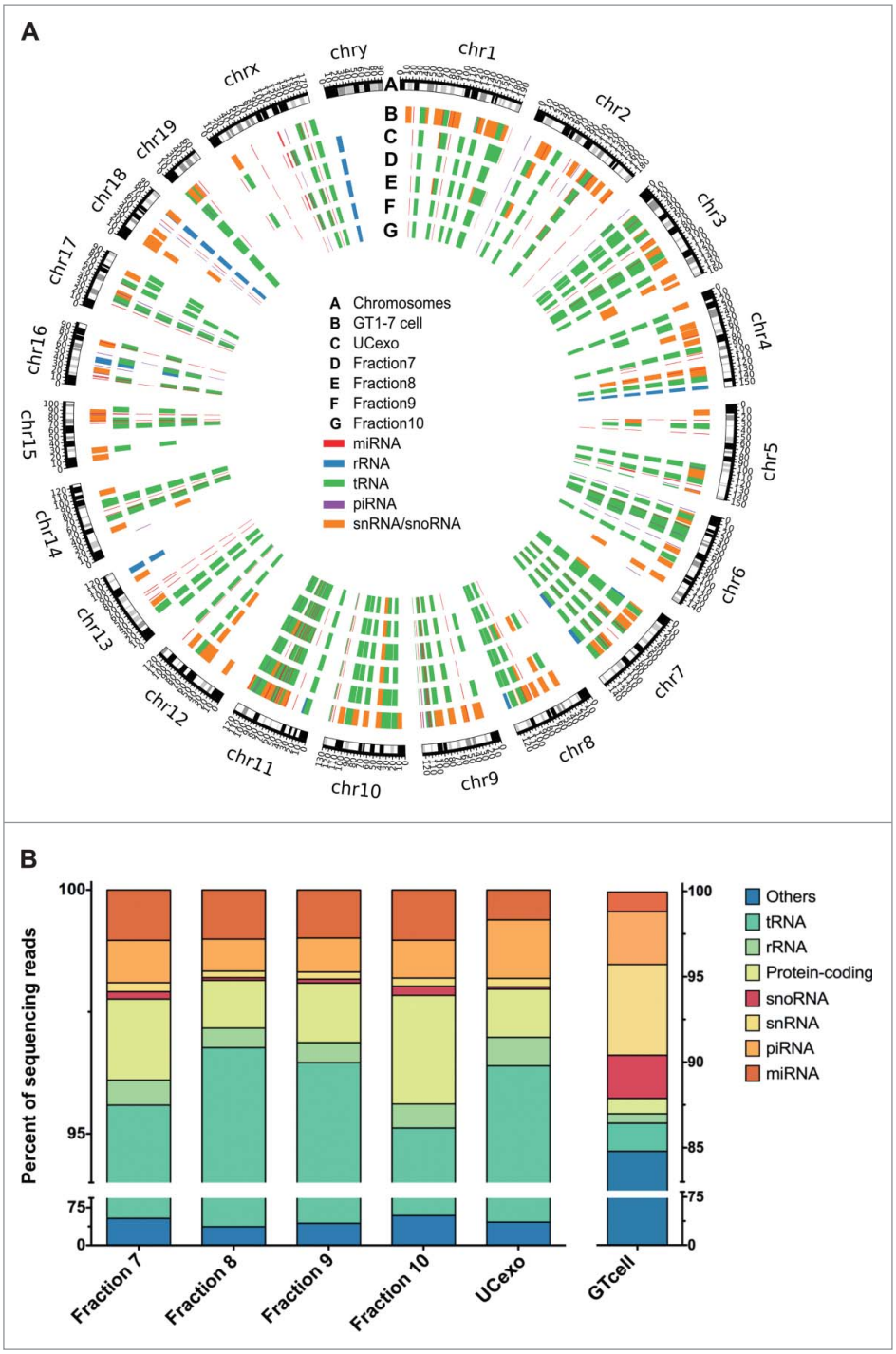

Figure 4. Small RNA sequencing of GT1–7 neuronal cells and GT1–7-derived exosomes isolated by 2 different protocols. (A) Circos diagram depicting small RNA transcriptome data. Track A: cytogenetic bands, chromosomes are depicted qter to pter. Track B to G: Highlight of all small RNAs (miRNA, rRNA, tRNA, piRNA, snRNA and snoRNA) identified across different sample groups in respect to GT1–7 neuronal cell, exosomes isolated from differential UC (protocol 1) and Optiprep fractions (i.e. Fraction 7 to 10) using Optiprep velocity gradient ultracentrifugation (protocol 2). (B) Distribution of small RNA species in the analyzed data sets. Profiles of different biotypes in each data set are percentage proportion to the total reads mapped to small RNA species and other elements, in particular to tRNA, rRNA, snoRNA, snRNA, piwi-RNA, miRNA, protein-coding fragments and others (i.e. repeat elements). Abbreviations: 'miRNA' – microRNA; 'rRNA' – rRNA; 'tRNA' – tRNA; 'piRNA' – piwi-interacting RNA; 'snRNA' – small nuclear RNA; 'snoRNA' – small nucleolar RNA; 'UCexo' – exosomes from differential UC.

range 0.11–0.23.%), snoRNA (median 0.07%, range 0.04–0.10%) and fragments of tRNA (median 54.3%, range 41.6–67.0%), rRNA (median 0.54%, range 0.20–0.88%) and protein-coding mRNA (range 0.49–1.82%) (Table 1 and Supplementary Table S2). The remaining ~42.26% sequences contained mostly fragments of RNA repeat elements. The collated results from the identified ncRNA species displayed that exosomes isolated from both methods consist of a diverse range of small RNA sequences.

Comparison of small RNA profiles in exosomes

The relationship of small ncRNAs was explored among samples to survey for any clustering of data sets. Three clusters were

Table 1. Total number of sequencing reads and percentage of each RNA biotype reads.

	Optiprep velocity gradient ultracentrifugation ($n = 5$)				Differential ultracentrifugation ($n = 3$)	Neuronal cell ($n = 3$)
	Fraction 7	Fraction 8	Fraction 9	Fraction 10	UCexo	GT1–7 cell
miRNA	1957 (1.03%)	5973 (1.01%)	2642 (0.99%)	1697 (1.03%)	4225 (0.62%)	6555 (1.12%)
piRNA	1822 (0.86%)	4255 (0.66%)	1884 (0.70%)	1365 (0.77%)	8500 (1.20%)	17513 (3.01%)
snRNA	402 (0.19%)	926 (0.13%)	395 (0.15%)	326 (0.17%)	1250 (0.17%)	30286 (5.16%)
snoRNA	244 (0.15%)	417 (0.05%)	211 (0.08%)	281 (0.19%)	327 (0.05%)	14268 (2.46%)
Protein-coding	3872 (1.66%)	7626 (0.98%)	3455 (1.22%)	3476 (2.23%)	7159 (0.99%)	5145 (0.87%)
rRNA	867 (0.51%)	2660 (0.40%)	1123 (0.41%)	757 (0.50%)	4166 (0.58%)	3136 (0.54%)
tRNA	112571 (42.01%)	455318 (59.66%)	141374 (52.68%)	84680 (35.86%)	366833 (50.27%)	9327 (1.60%)

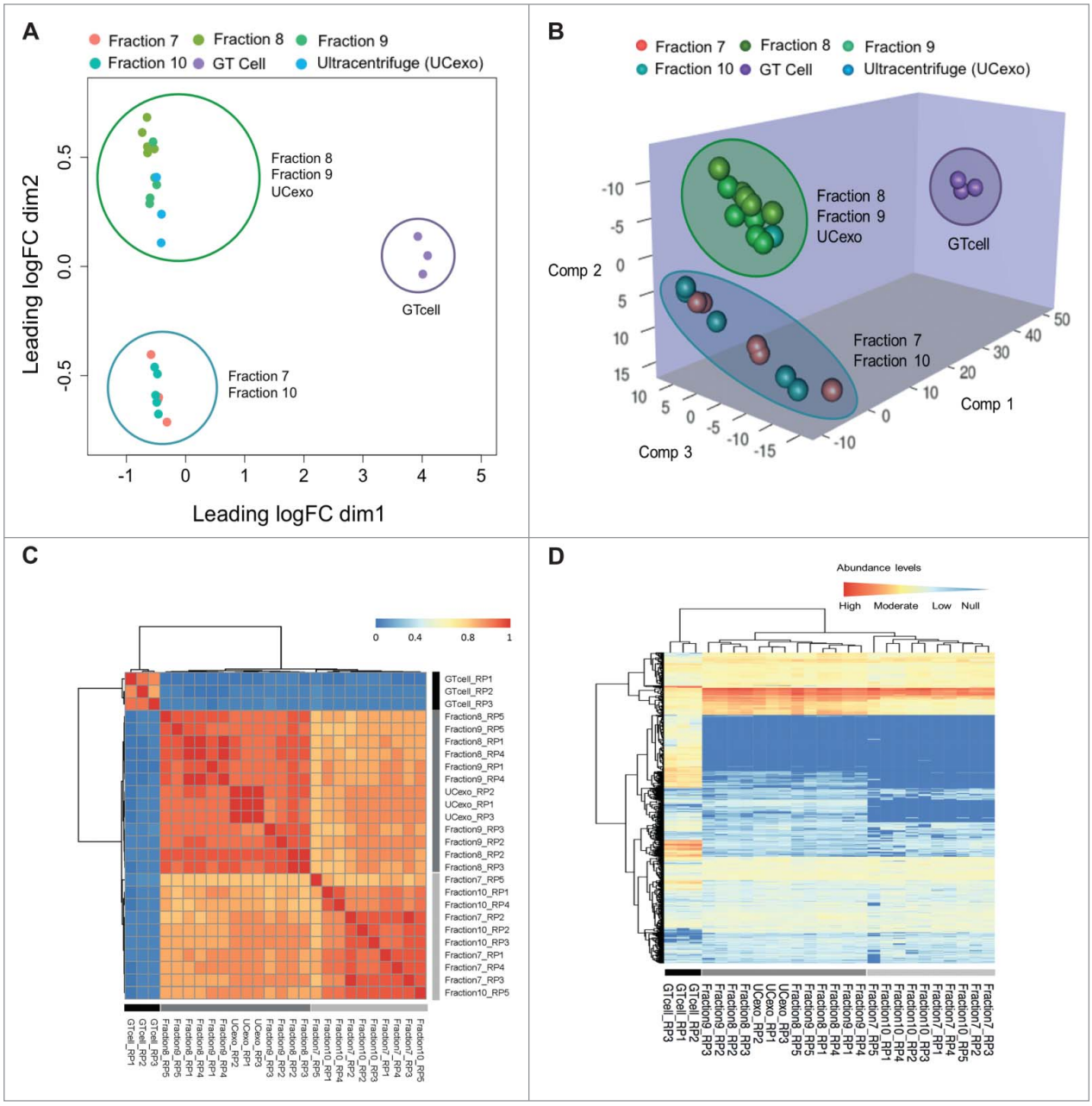

Figure 5. The relationship of small RNA expression profiles among the samples. (A) Multidimensional scaling plot demonstrating the clustering of replicates in each data set, with the vertical axis corresponding to the logarithm base 2 (log2) fold change (FC) in dimensional (dim) 2 and the horizontal axis showing log2FC dim 1. (B) Three-dimensional principal component analysis further depicting the clustering of sample replicates among the data sets. The x-, y- and z- axis represents first, second and third principal component of small RNA data. (C) Distance mapping of small RNA expression using Euclidean distance metric of Optiprep fractions, UC exosomes (UCexo) samples and GT1–7 neuronal cells. Exosomes Optiprep fractions (i.e. Fraction 8 and 9) and UCexo are closely related to each other but distantly related to GT1–7 neuronal cells. Exosomes Optiprep fraction 7 (excluding replicate 5 from fraction 7) and 10 are closely related to each other as compared with exosomes samples, but distantly related to GT1–7 neuronal cells. The correlation value is represented by the color ranging from blue (0 to 0.4) to yellow (0.41 to 0.79) to red (0.8 to 1). (D) Heatmap of unsupervised hierarchical clustering of normalized small RNA expression. The degree of low to high expression is represented by a range of color starting from blue to yellow to red, indicating the absence or presence of RNA. Abbreviation: 'UCexo' – exosomes isolated from differential UC.

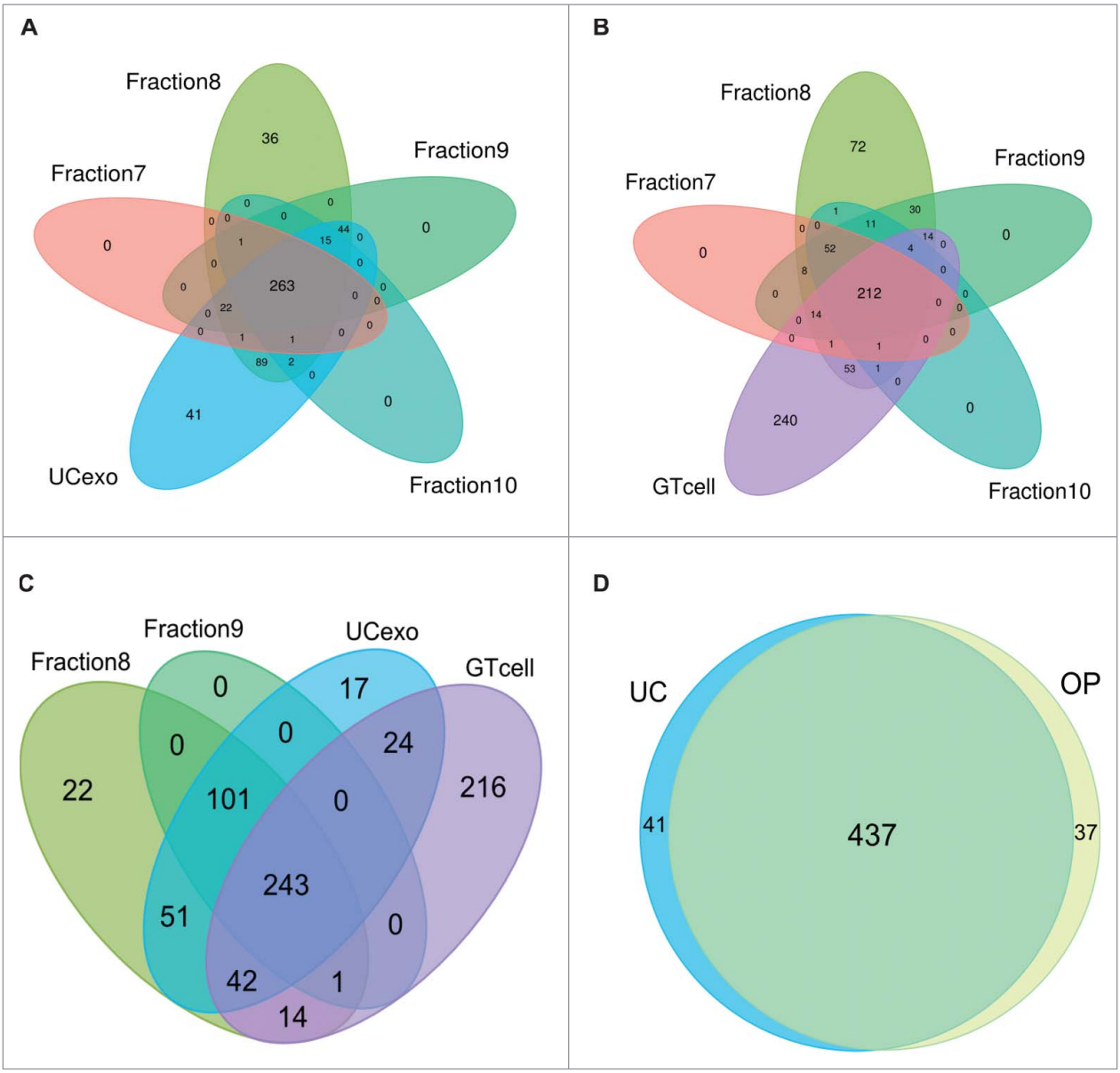

Figure 6. Venn diagrams showing unique and common small RNA detected in different exosome methods and GT1–7 neuronal cells. (A) The 5-way Venn diagram illustrates the differences and similarities of small RNAs identified in exosomes isolated from differential UC method (protocol 1) and Optiprep velocity gradient ultracentrifugation (protocol 2). (B) The 5-way Venn diagram demonstrates the overlapping of small RNAs across all fractions with enriched small RNA in Fraction 8 and 9. (C) The 4-way Venn diagram displays the unique small RNA in exosome data sets when compared with GT1–7 neuronal cells. (D) The proportional Venn diagram demonstrates the similarities of small RNA extracted from both protocols. Please see list of small RNAs across Venn diagrams in Supplementary File 1.

observed in the MDS and PCA plot with dominant clusters as cells, exosomes and other Optiprep fractions (Fig. 5A and B). In addition to the MDS and PCA plots, the correlation between the replicates of each data set were explored. The distance mapping by Euclidean distance metric (Fig. 5C) demonstrated that replicates were highly correlated; Spearman's correlation coefficients ranging from 0.8 to 0.9 for each data set (Fig. S2), in which exosomes from Optiprep and differential UC were closely associated ($r = 0.94$). The unsupervised hierarchical clustering analysis (Fig. 5D) on log2-normalized reads also illustrated the distinct profile of small RNAs in exosomes. The individual profiles of small RNAs are shown in Fig. S3. The expression profile analysis provided an initial verification that both methods were capable of isolating exosomes with similar small RNA profiles.

To investigate in greater detail the small RNA profiles in exosomes isolated from the two different methods, small RNAs that were unique or common to the different preparation protocols were examined. Across all the different small RNA species in Optiprep fractions, 263 small RNAs overlapped between the four fractions and UC exosomes, with 41 small RNAs that were unique in the UC exosomes (Fig. 6A). By comparing the RNA biotypes identified in Optiprep and UC exosomes with cells, 243 RNAs were in common, indicating that exosomes contained a unique subset of RNA from that of cells (Fig. 6B and C). A high proportion of other small RNAs were common between the small RNA profiles of exosomes isolated from the two methods (Fig. 6D).

To assess the small RNA profiles in the exosomes, the top small RNAs across the samples were tabulated in a matrix table (Fig. S4). The majority of miRNAs in exosomes was composed

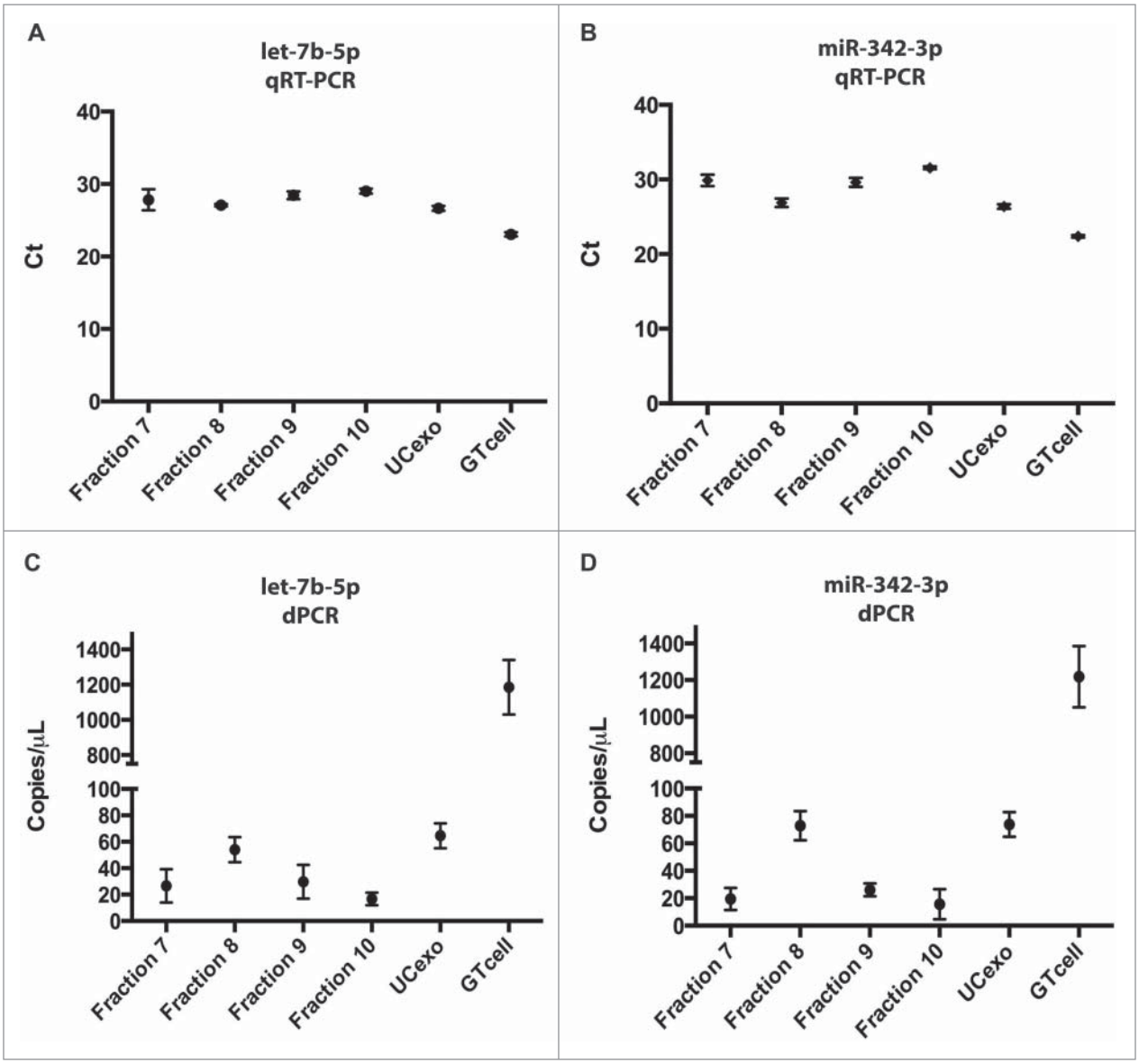

Figure 7. Validation of miRNA expression by qRT-PCR and digital PCR assays. qRT-PCR miRNA expression assays of GT1–7 cells and exosomes from differential UC (UCexo) and Optiprep fractions 7, 8, 9 and 10 for (A) let-7b and (B) miR-342-3p, data expressed as raw Ct values, n = 3. Digital PCR of miRNA in GT1–7 cells and exosomes from differential UC (UCexo) and Optiprep fractions 7, 8, 9 and 10 for let-7b (C) and miR-342-3p (D), data expressed as copies per μL, n = 3. Standard deviations are shown in the graph.

of let-7 gene family. Another miRNA of interest was miR-342-3p due to its presence in various diseased states.[8] To validate the NGS data we used targeted primer based technologies, qRT-PCR (Fig. 7A and B) and digital PCR (Fig. 7C and D), to confirm the presence of let-7b and miR-342–3p expression. Both primer based technologies displayed Ct values indicating a peak in abundance of let-7b and miR-342–3p with purified exosomes in Optiprep fraction 8, with similar expression observed for UC exosomes, confirming the observations seen in the NGS data. The small proportion of rRNA detected in exosomes composed of mostly 5S rRNA sequences of different variety, which was consistent with our published report.[8] Further, other small RNAs such as piRNA, snoRNA and snRNA were expressed in neuronal cell-derived exosomes, particularly the exosomes prepared by Optiprep, but little is known about their functional roles of piRNA in exosomes.

Specific tRNA fragments are identified in exosomes

Recently, studies have reported that the production of tRNA fragments were composed of tRNA halves (30–35 nt) and tRNA-derived fragments (13 and 20 nt in size).[43] These tRNA fragments were observed in our present study. In Fig. 8A, a large proportion of reads were observed to map to tRNA regions in exosomal samples which mostly comprised of tRNA fragments. The percentage composition of tRNA fragments (Fig. 8B and Fig. S5) showed that tRNA-Gly, tRNA-Lys and tRNA-Val isoacceptor type were abundant in exosome samples and the majority of these tRNA fragments range between 50–53 nt in length (Fig. 8C and D), except for tRNA-Lys where fragment lengths varied (Fig. 8E). Specific tRNAs appeared to be selectively loaded into exosomes as fragments.

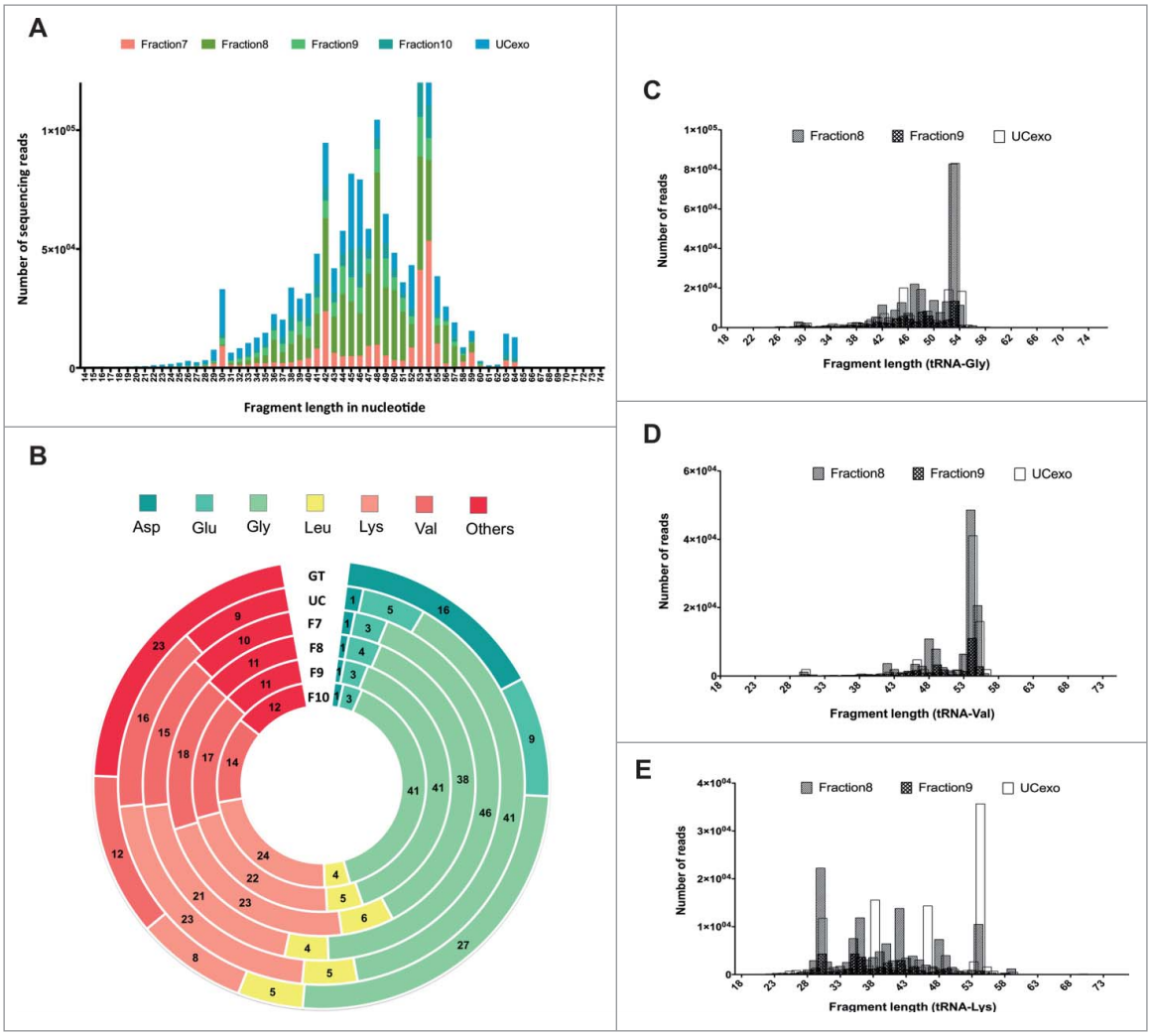

Figure 8. Exosomes contain tRNAs. (A) Histogram of transferRNA (tRNA) fragment lengths in nucleotides for tRNA-Gly, tRNA-Lys and tRNA-Val in all data sets. (B) Percentage composition of the tRNA isoacceptor type showing abundancy of tRNA-Gly, tRNA-Lys and tRNA-Val. The doughnut chart illustrates the distribution of different tRNA isoacceptor types. Percentage reads mapping to each type are average across the replicates in each data set. (C) Histogram of tRNA smaller fragments in exosome data sets (i.e. exosomes from differential UC (UCexo) and Optiprep fraction 8 and 9). The bar shows peaks between 53 and 56 nucleotides.

Discussion

There has been a particular interest in determining the most appropriate method for purifying exosomes to profile small RNA.[8,12,44] Studies have demonstrated that exosomes provide a protective and enriched source of small RNA for disease biomarker detection in biologic specimens.[19,45-48] The method to isolate exosomes is often selected based on the ability to minimise co-purifying protein aggregates and other extracellular particles. The minimisation of such contaminating elements may provide the opportunity to perform further downstream analyses, such as structural biology, proteomics, lipidomics and genomics. In this study, we investigated the need for a more defined method for small RNA profiling.

Here, we have applied the two common protocols that were previously published for isolating GT1–7 neuronal cell-derived exosomes.[8,23,29] Differential UC (protocol 1) is the most conventionally used technique to isolate exosomes from GT1–7 cells and other cell lines. However, UC technique is limiting in the ability to minimise contaminating proteins and other membranous particles. More specific separation methods, particularly over a gradient is necessary for studies requiring increased purity of exosomes. Optiprep velocity gradients (protocol 2) were previously demonstrated by Coleman et al. to further purify exosome preparations devoid of contaminating elements that may hinder downstream analysis as observed by high-resolution microscopy. To perform a comprehensive survey of small RNA species in exosomes isolated from each method, a high-throughput workflow that comprised of NGS and bioinformatics was used. Sequence reads were mapped to loci of a wide variety of small ncRNA species, such as miRNA, piRNA, tRNA rRNA, snoRNA and snRNA. The expression analysis of exosomes prepared by both methods suggested that the small RNA profiles of exosomes were similar to each other and distinct from the GT1–7 neuronal cells. The overall RNA composition in exosomes further confirmed our previous study investigating small RNA profiles in circulating exosomes released from prion-infected GT1–7 neuronal cells.[8]

As miRNAs are sorted into exosomes and secreted into the bloodstream there is an interest in profiling for miRNA disease associated signatures in exosomes.[19,22,44] Disease signatures have comprised of miRNAs such as miR-29b, miR-342–3p,

miR-424 and let-7 family which were dysregulated in neurodegenerative diseases including Alzheimer and Prion diseases.[9,42,49] In this study, we successfully validated the presence of let-7b-5p and miR-342-3p in UC exosomes and Optiprep purified exosomes via qRT-PCR and digital PCR suggesting that Optiprep gradients are not required to detect these miRNAs for biomarker purposes. Among these miRNAs, the top miRNA signatures presented in exosomes prepared by both methods mostly overlapped thus, both Optiprep gradient and UC methods are capable of isolating exosomes that contained similar miRNA profiles. Further, these miRNAs exhibited neuronal signaling regulation such as neurologic development and differentiation,[8,9,42] suggesting the potential functional role of exosomes implicated in neurologic processes.

Recently, studies have demonstrated that the biogenesis of tRNA fragments serves a specific process depending on the cell type and cellular condition.[50,51] Fragments derived from tRNA were found to be specifically cleaved to perform diverse functions, such as reverse transcription and guidance of other RNAs.[52-54] There are two main groups of tRNA fragments; tRNA halves (30–35 nt) and tRNA-derived fragments (30–50 nt).[43] Furthermore, specific coverage of the fragments on the 3′ or 5′ end of tRNA had different functional roles. For example, 3′ tRNA fragments have been found to be associated with Argonaute proteins and potentially function similarly to miRNA by repressing translation. Our study displayed a large number of sequences mainly composed of ~30–53 nt tRNA-derived fragments in exosomes. Upon analyzing the abundant tRNA in exosomes, tRNA-Gly isotypes were mostly derived from the 3′ end (Fig. S6). Given the potential for tRNA fragments to play important roles in regulating many biologic processes, further studies on the selective abundance of specific types of tRNA fragments in exosomes are necessary to elucidate the current finding.

Using NGS, exosomes prepared by both methods were observed to contain a significant expression of piRNAs. piRNAs are of 24–32 nt in length and associate with Piwi family of proteins including MIWI, MILI, and MIWI2.[55] Initially, piRNA were reported to be implicated in silencing transposable elements of an animal germ line.[56-58] The first evidence demonstrating the presence of piRNA in the nervous system was reported by Lee et al., in which piRNA complexes were found to be implicated in dendritic spine development of axons.[59] In this study, a panel of piRNAs found in exosomes may assist in the shuttle of piRNA between cells to act upon their targets within a neuronal system. Other small RNAs detected were snRNAs or snoRNAs, based on their average size (60–300 nt), however there was a low abundance of these transcripts. Although sn/snoRNAs have been shown to regulate transcription factors and translation.[60,61] the exact mechanism still requires further investigation. The silencing and other potential functions from these ncRNA species may provide additional mechanisms and further understanding exosomal cargo and transfer.

A noteworthy contrast of this study is one performed by Van Deun et al where they observed distinct mRNA profiles obtained from microarray analysis of exosomes isolated from UC and Optiprep.[62] The contrast of our studies may be due to slight differences in exosomal isolation methods and our ability to obtain high unbiased deep sequencing coverage of small RNA which demonstrated that exosomes can contain larger amounts of small RNA between 20 to 200 nt in length.

In conclusion, the use of high throughput workflow revealed a wealth of information on the different biotypes of small ncRNAs in exosomes prepared by Optiprep gradient and UC method. Similar exosomal small RNA profiles from both exosome isolation methods are demonstrated in the present study, suggesting that the presence of remaining cell debris does not influence downstream transcriptomic analysis, in particular, for the detection of small RNA biomarkers. The UC method may be the preferred protocol as it provides a time efficient and easy protocol for small RNA biomarker discovery projects and further applications.

Disclosure of potential conflicts of interest

No potential conflicts of interest were disclosed.

Acknowledgements

We thank the Life Sciences Computation Center of Victorian Life Sciences Computation Initiative, an initiative of the Victorian Government, Australia hosted at the University of Melbourne, for high-performance computing system and resources.

Funding

This work was supported by grants from the Australian Research Council (FT100100560 to AFH), the National Health and Medical Research Council (628946 to AFH), Belberry Indigenous Health Fellowships (MDHS, The University of Melbourne) to S.A.B. C.Q. was supported by Melbourne International Research Scholarship.

ORCID

Camelia Quek http://orcid.org/0000-0002-1244-961X
Chol-Hee Jung http://orcid.org/0000-0002-2992-3162
Andrew F. Hill http://orcid.org/0000-0001-5581-2354

References

1. Eddy SR. Non-coding RNA genes and the modern RNA world. Nat Rev Genet 2001; 2:919-929; PMID:11733745; http://dx.doi.org/10.1038/35103511
2. Mattick JS, Makunin IV. Non-coding RNA. Hum Mol Genet 2006; 15 (Spec No 1):R17-29; PMID:16651366; http://dx.doi.org/10.1093/hmg/ddl046
3. Bartel DP. MicroRNAs: genomics, biogenesis, mechanism, and function. Cell 2004; 116:281-297; PMID:14744438; http://dx.doi.org/10.1016/S0092-8674(04)00045-5
4. Baek D, Villen J, Shin C, Camargo FD, Gygi SP, Bartel DP. The impact of microRNAs on protein output. Nature 2008; 455:64-71; PMID:18668037; http://dx.doi.org/10.1038/nature07242
5. Zuo Z, Maiti S, Hu SM, Loghavi S, Calin GA, Garcia-Manero G, Kantarjian HM, Medeiros LJ, Cooper LJN, Bueso-Ramos CE. Plasma circulating-microRNA profiles are useful for assessing prognosis in patients with cytogenetically normal myelodysplastic syndromes. Modern Pathology 2015; 28:373-382; PMID:25216221; http://dx.doi.org/10.1038/modpathol.2014.108
6. Hales CM, Seyfried NT, Dammer EB, Duong D, Yi H, Gearing M, Troncoso JC, Mufson EJ, Thambisetty M, Levey AI, et al. U1 small nuclear ribonucleoproteins (snRNPs) aggregate in Alzheimer's disease due to autosomal dominant genetic mutations and trisomy 21. Mol

Neurodegener 2014; 9:15-21; PMID:24773620; http://dx.doi.org/10.1186/1750-1326-9-15
7. Finnegan EJ, Matzke MA. The small RNA world. J Cell Sci 2003; 116:4689-4693; PMID:14600255; http://dx.doi.org/10.1242/jcs.00838
8. Bellingham SA, Coleman BM, Hill AF. Small RNA deep sequencing reveals a distinct miRNA signature released in exosomes from prion-infected neuronal cells. Nucleic Acids Res 2012; 40:10937-10949; PMID:22965126; http://dx.doi.org/10.1093/nar/gks832
9. Saba R, Goodman CD, Huzarewich R, Robertson C, Booth SA. A miRNA Signature of Prion Induced Neurodegeneration. PLoS One 2008; 3:e3652; PMID:18987751; http://dx.doi.org/10.1371/journal.pone.0003652
10. Faghihi MA, Modarresi F, Khalil AM, Wood DE, Sahagan BG, Morgan TE, Finch CE, Laurent GS, Kenny PJ, Wahlestedt C. Expression of a noncoding RNA is elevated in Alzheimer's disease and drives rapid feed-forward regulation of beta-secretase. Nat Med 2008; 14:723-730; PMID:18587408; http://dx.doi.org/10.1038/nm1784
11. Xue W, Dahlman JE, Tammela T, Khan OF, Sood S, Dave A, Cai WX, Chirino LM, Yang GR, Bronson R, et al. Small RNA combination therapy for lung cancer. Proc Natl Acad Sci U S A 2014; 111:E3553-E3561; PMID:25114235; http://dx.doi.org/10.1073/pnas.1412686111
12. Volinia S, Galasso M, Sana ME, Wise TF, Palatini J, Huebner K, Croce CM. Breast cancer signatures for invasiveness and prognosis defined by deep sequencing of microRNA. Proc Natl Acad Sci U S A 2012; 109:3024-3029; PMID:22315424; http://dx.doi.org/10.1073/pnas.1200010109
13. Liu R, Zhang CN, Hu ZB, Li G, Wang C, Yang CH, Huang DZ, Chen X, Zhang HY, Zhuang R, et al. A 5-microRNA signature identified from genome-wide serum microRNA expression profiling serves as a fingerprint for gastric cancer diagnosis. European J Cancer 2011; 47:784-791; PMID:21112772; http://dx.doi.org/10.1016/j.ejca.2010.10.025
14. Kurowska-Stolarska M, Alivernini S, Ballantine LE, Asquith DL, Millar NL, Gilchrist DS, Reilly J, Ierna M, Fraser AR, Stolarski B, et al. MicroRNA-155 as a proinflammatory regulator in clinical and experimental arthritis. Proc Natl Acad Sci U S A 2011; 108:11193-11198; PMID:21690378; http://dx.doi.org/10.1073/pnas.1019536108
15. De Felice B, Mondola P, Sasso A, Orefice G, Bresciamorra V, Vacca G, Biffali E, Borra M, Pannone R. Small non-coding RNA signature in multiple sclerosis patients after treatment with interferon-beta. BMC Med Genomics 2014; 7:26; PMID:24885345; http://dx.doi.org/10.1186/1755-8794-7-26
16. Bellingham SA, Guo BB, Coleman BM, Hill AF. Exosomes: vehicles for the transfer of toxic proteins associated with neurodegenerative diseases? Front Physiol 2012; 3:124; PMID:22563321; http://dx.doi.org/10.3389/fphys.2012.00124
17. Valadi H, Ekstrom K, Bossios A, Sjostrand M, Lee JJ, Lotvall JO. Exosome-mediated transfer of mRNAs and microRNAs is a novel mechanism of genetic exchange between cells. Nat Cell Biol 2007; 9:654-659; PMID:17486113; http://dx.doi.org/10.1038/ncb1596
18. Keller S, Ridinger J, Rupp AK, Janssen JW, Altevogt P. Body fluid derived exosomes as a novel template for clinical diagnostics. J Transl Med 2011; 9:86; PMID:21651777; http://dx.doi.org/10.1186/1479-5876-9-86
19. Cheng L, Sharples RA, Scicluna BJ, Hill AF. Exosomes provide a protective and enriched source of miRNA for biomarker profiling compared to intracellular and cell-free blood. J Extracell Vesicles 2014; 3:124; PMID:24683445; http://dx.doi.org/10.3402/jev.v3.23743
20. Tauro BJ, Greening DW, Mathias RA, Ji H, Mathivanan S, Scott AM, Simpson RJ. Comparison of ultracentrifugation, density gradient separation, and immunoaffinity capture methods for isolating human colon cancer cell line LIM1863-derived exosomes. Methods 2012; 56:293-304; PMID:22285593; http://dx.doi.org/10.1016/j.ymeth.2012.01.002
21. Cheng L, Sun X, Scicluna BJ, Coleman BM, Hill AF. Characterization and deep sequencing analysis of exosomal and non-exosomal miRNA in human urine. Kidney Int 2014; 86:433-444; PMID:24352158; http://dx.doi.org/10.1038/ki.2013.502
22. Crescitelli R, Lasser C, Szabo TG, Kittel A, Eldh M, Dianzani I, Buzas EI, Lotvall J. Distinct RNA profiles in subpopulations of extracellular vesicles: apoptotic bodies, microvesicles and exosomes. J Extracell Vesicles 2013; 2; PMID:24223256; http://dx.doi.org/10.3402/jev.v2i0.20677
23. Coleman BM, Hanssen E, Lawson VA, Hill AF. Prion-infected cells regulate the release of exosomes with distinct ultrastructural features. FASEB J 2012; 26:4160-4173; PMID:22767229; http://dx.doi.org/10.1096/fj.11-202077
24. Shaw ML, Stone KL, Colangelo CM, Gulcicek EE, Palese P. Cellular proteins in influenza virus particles. Plos Pathogens 2008; 4:e1000085; PMID:18535660; http://dx.doi.org/10.1371/journal.ppat.1000085
25. Pritchard CC, Cheng HH, Tewari M. MicroRNA profiling: approaches and considerations. Nat Rev Genet 2012; 13:358-369; PMID:22510765; http://dx.doi.org/10.1038/nrg3198
26. Klein D. Quantification using real-time PCR technology: applications and limitations. Trends Mol Med 2002; 8:257-260; PMID:12067606; http://dx.doi.org/10.1016/S1471-4914(02)02355-9
27. Cheng L, Quek CY, Sun X, Bellingham SA, Hill AF. The detection of microRNA associated with Alzheimer's disease in biological fluids using next-generation sequencing technologies. Front Genet 2013; 4:150; PMID:23964286; http://dx.doi.org/10.3389/fgene.2013.00150
28. Quek C, Jung CH, Bellingham SA, Lonie A, Hill AF. iSRAP - a one-touch research tool for rapid profiling of small RNA-seq data. J Extracell vesicles 2015; 4:29454; PMID:26561006; http://dx.doi.org/10.3402/jev.v4.29454
29. Vella LJ, Sharples RA, Lawson VA, Masters CL, Cappai R, Hill AF. Packaging of prions into exosomes is associated with a novel pathway of PrP processing. J Pathol 2007; 211:582-590; PMID:17334982; http://dx.doi.org/10.1002/path.2145
30. Griffiths-Jones S, Grocock RJ, van Dongen S, Bateman A, Enright AJ. miRBase: microRNA sequences, targets and gene nomenclature. Nucleic Acids Res 2006; 34:D140-144; PMID:16381832; http://dx.doi.org/10.1093/nar/gkj112
31. Chan PP, Lowe TM. GtRNAdb: a database of transfer RNA genes detected in genomic sequence. Nucleic Acids Res 2009; 37:D93-97; PMID:18984615; http://dx.doi.org/10.1093/nar/gkn787
32. Sai Lakshmi S, Agrawal S. piRNABank: a web resource on classified and clustered Piwi-interacting RNAs. Nucleic Acids Res 2008; 36:D173-177; PMID:17881367; http://dx.doi.org/10.1093/nar/gkm696
33. Robinson MD, McCarthy DJ, Smyth GK. edgeR: a Bioconductor package for differential expression analysis of digital gene expression data. Bioinformatics 2010; 26:139-140; PMID:19910308; http://dx.doi.org/10.1093/bioinformatics/btp616
34. Kolde R. Pheatmap: pretty heatmaps. R package version 0.7 2012; 4.
35. Leinonen R, Akhtar R, Birney E, Bower L, Cerdeno-Tarraga A, Cheng Y, Cleland I, Faruque N, Goodgame N, Gibson R, et al. The European Nucleotide Archive. Nucleic Acids Res 2011; 39:D28-31; PMID:20972220; http://dx.doi.org/10.1093/nar/gkq967
36. Krzywinski M, Schein J, Birol I, Connors J, Gascoyne R, Horsman D, Jones SJ, Marra MA. Circos: an information aesthetic for comparative genomics. Genome Res 2009; 19:1639-1645; PMID:19541911; http://dx.doi.org/10.1101/gr.092759.109
37. Cao KAL, Boitard S, Besse P. Sparse PLS discriminant analysis: biologically relevant feature selection and graphical displays for multiclass problems. BMC Bioinformatics 2011; 12:253; PMID:21693065; http://dx.doi.org/10.1186/1471-2105-12-253
38. Carey RN, Wold S, Westgard JO. Principal component analysis: an alternative to "referee" methods in method comparison studies. Analytical Chem 1975; 47:1824-1829; PMID:1163784; http://dx.doi.org/10.1021/ac60361a037
39. Wilkinson L, Urbanek S Venneuler: Venn and Euler Diagrams. R package version 1.1 2011; http://www.rforge.net/venneuler
40. Warnes GR, Bolker B, Bonebakker L, Gentleman R, Huber W, Liaw A, Lumley T, Maechler M, Magnusson A, Moeller S. gplots: Various R programming tools for plotting data. R package version 2009; 2; https://cran.r-project.org/package=gplots

41. Schatzl HM, Laszlo L, Holtzman DM, Tatzelt J, DeArmond SJ, Weiner RI, Mobley WC, Prusiner SB. A hypothalamic neuronal cell line persistently infected with scrapie prions exhibits apoptosis. J Virol 1997; 71:8821-8831; PMID:9343242
42. Montag J, Hitt R, Opitz L, Schulz-Schaeffer WJ, Hunsmann G, Motzkus D. Upregulation of miRNA hsa-miR-342-3p in experimental and idiopathic prion disease. Mol Neurodegener 2009; 4:36; PMID:19712440; http://dx.doi.org/10.1186/1750-1326-4-36
43. Lee YS, Shibata Y, Malhotra A, Dutta A. A novel class of small RNAs: tRNA-derived RNA fragments (tRFs). Gen Dev 2009; 23:2639-2649; PMID:19933153; http://dx.doi.org/10.1101/gad.1837609
44. Cheng L, Doecke JD, Sharples RA, Villemagne VL, Fowler CJ, Rembach A, Martins RN, Rowe CC, Macaulay SL, Masters CL, et al. Prognostic serum miRNA biomarkers associated with Alzheimer's disease shows concordance with neuropsychological and neuroimaging assessment. Mol Psychiatry 2015; 20(10):1188-96; PMID:25349172; http://dx.doi.org/10.1038/mp.2014.127
45. Skog J, Wurdinger T, van Rijn S, Meijer DH, Gainche L, Sena-Esteves M, Curry WT, Carter BS, Krichevsky AM, Breakefield XO. Glioblastoma microvesicles transport RNA and proteins that promote tumour growth and provide diagnostic biomarkers. Nat Cell Biol 2008; 10:1470-U1209; PMID:19011622; http://dx.doi.org/10.1038/ncb1800
46. Miranda KC, Bond DT, McKee M, Skog J, Paunescu TG, Da Silva N, Brown D, Russo LM. Nucleic acids within urinary exosomes/microvesicles are potential biomarkers for renal disease. Kidney Int 2010; 78:191-199; PMID:20428099; http://dx.doi.org/10.1038/ki.2010.106
47. Lasser C, Alikhani VS, Ekstrom K, Eldh M, Paredes PT, Bossios A, Sjostrand M, Gabrielsson S, Lotvall J, Valadi H. Human saliva, plasma and breast milk exosomes contain RNA: uptake by macrophages. J Translat Med 2011; 9; PMID:21235781; http://dx.doi.org/10.1186/1479-5876-9-9
48. Li M, Zeringer E, Barta T, Schageman J, Cheng AG, Vlassov AV. Analysis of the RNA content of the exosomes derived from blood serum and urine and its potential as biomarkers. Philos Trans R Soc B-Biol Sci 2014; 369:20130502; PMID:25135963; http://dx.doi.org/10.1098/rstb.2013.0502
49. Wang WX, Huang QW, Hu YL, Stromberg AJ, Nelson PT. Patterns of microRNA expression in normal and early Alzheimer's disease human temporal cortex: white matter versus gray matter. Acta Neuropathologica 2011; 121:193-205; PMID:20936480; http://dx.doi.org/10.1007/s00401-010-0756-0
50. Wang QR, Lee I, Ren JP, Ajay SS, Lee YS, Bao XY. Identification and Functional Characterization of tRNA-derived RNA Fragments (tRFs) in Respiratory Syncytial Virus Infection. Mol Ther 2013; 21:368-379; PMID:23183536; http://dx.doi.org/10.1038/mt.2012.270
51. Dhahbi JM, Spindler SR, Atamna H, Yamakawa A, Boffelli D, Mote P, Martin DIK. 5′ tRNA halves are present as abundant complexes in serum, concentrated in blood cells, and modulated by aging and calorie restriction. BMC Genomics 2013; 14:298; PMID:23638709; http://dx.doi.org/10.1186/1471-2164-14-298
52. Hurto RL. Unexpected Functions of tRNA and tRNA Processing Enzymes. Adv Exp Med Biol 2011; 722:137-155; PMID:21915787; http://dx.doi.org/10.1007/978-1-4614-0332-6_9
53. Anderson P, Ivanov P. tRNA fragments in human health and disease. FEBS Lett 2014; 588:4297-304; PMID:25220675; http://dx.doi.org/10.1016/j.febslet.2014.09.001
54. Abbott JA, Francklyn CS, Robey-Bond SM. Transfer RNA and human disease. Front Genet 2014; 5:158; PMID:24917879; http://dx.doi.org/10.3389/fgene.2014.00158
55. Vourekas A, Zheng Q, Alexiou P, Maragkakis M, Kirino Y, Gregory BD, Mourelatos Z. Mili and Miwi target RNA repertoire reveals piRNA biogenesis and function of Miwi in spermiogenesis. Nat Struct Mol Biol 2012; 19:773-781; PMID:22842725; http://dx.doi.org/10.1038/nsmb.2347
56. Castaneda J, Genzor P, Bortvin A. piRNAs, transposon silencing, and germline genome integrity. Mutation Res 2011; 714:95-104; PMID:21600904; \http://dx.doi.org/10.1016/j.mrfmmm.2011.05.002
57. Dufourt J, Dennis C, Boivin A, Gueguen N, Theron E, Goriaux C, Pouchin P, Ronsseray S, Brasset E, Vaury C. Spatio-temporal requirements for transposable element piRNA-mediated silencing during Drosophila oogenesis. Nucleic Acids Res 2014; 42:2512-2524; PMID:24288375; http://dx.doi.org/10.1093/nar/gkt1184
58. Chambeyron S, Popkova A, Payen-Groschene G, Brun C, Laouini D, Pelisson A, Bucheton A. piRNA-mediated nuclear accumulation of retrotransposon transcripts in the Drosophila female germline. Proc Natl Acad Sci U S A 2008; 105:14964-14969; PMID:18809914; http://dx.doi.org/10.1073/pnas.0805943105
59. Lee EJ, Banerjee S, Zhou H, Jammalamadaka A, Arcila M, Manjunath BS, Kosik KS. Identification of piRNAs in the central nervous system. RNA 2011; 17:1090-1099; PMID:21515829; http://dx.doi.org/10.1261/rna.2565011
60. Matera AG, Terns RM, Terns MP. Non-coding RNAs: lessons from the small nuclear and small nucleolar RNAs. Nat Rev Mol Cell Biol 2007; 8:209-220; PMID:17318225; http://dx.doi.org/10.1038/nrm2124
61. Kiss T. Biogenesis of small nuclear RNPs. J Cell Sci 2004; 117:5949-5951; PMID:15564372; http://dx.doi.org/10.1242/jcs.01487
62. Van Deun J, Mestdagh P, Sormunen R, Cocquyt V, Vermaelen K, Vandesompele J, Bracke M, De Wever O, Hendrix A. The impact of disparate isolation methods for extracellular vesicles on downstream RNA profiling. J Extracell Vesicles 2014; 3; PMID:25317274; http://dx.doi.org/10.3402/jev.v3.24858